

Temperature-Induced Bifurcations in the Cu(II)-Catalyzed and Catalyst-Free Hydrogen Peroxide-Thiosulfate Oscillating Reaction

Ling Yuan,[†] Qingyu Gao,^{*,†,‡} Yuemin Zhao,[†] Xiaodong Tang,[†] and Irving R. Epstein^{*,‡}

College of Chemical Engineering, China University of Mining and Technology, Xuzhou 221008 China and Department of Chemistry and Volen Center for Complex Systems, MS 015, Brandeis University, Waltham, Massachusetts 02454-9110

Received: March 5, 2010; Revised Manuscript Received: May 20, 2010

We study the oxidation dynamics of thiosulfate ions by hydrogen peroxide in the presence of trace amounts of copper(II) using the reaction temperature as a control parameter in a continuous flow stirred tank reactor. The system displays period-doubling, aperiodic, and mixed-mode oscillations at different temperatures. We are able to simulate these complex dynamics with a model proposed by Kurin-Csörgei et al. The model suggests that the Cu²⁺-containing term is not essential for the observed oscillations. We find small-amplitude and high-frequency oscillations in the catalyst-free experimental system. The reaction between H₂O₂ and S₂O₃²⁻ contains the core mechanism of the H₂O₂–S₂O₃²⁻–Cu²⁺ and H₂O₂–S₂O₃²⁻–SO₃²⁻ oscillatory systems, while the Cu²⁺ and SO₃²⁻ modulate the feedback loops so as to strengthen the oscillatory dynamics.

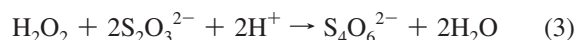
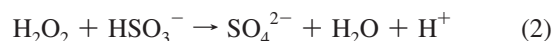
I. Introduction

Nonlinear oscillatory dynamics is ubiquitous in biological and physiological systems.^{1,2} Chemical reaction systems are more easily studied and controlled in the laboratory and hence are likely to provide more systematic insights into the fundamental mechanisms leading to complex spatiotemporal dynamics. A number of chemical oscillators have been designed and studied systematically by using simple composite reactions as building blocks. Among them, pH oscillators constitute the largest family of chemical reaction systems found to oscillate in a continuous flow stirred tank reactor (CSTR).³ In the family of pH oscillators, which can induce changes in key physiological parameters, H⁺ serves as the autocatalytic species. Thus, such potential applications for pH oscillators have been proposed as artificial muscles,^{4,5} controlled drug-delivery systems,⁶ and DNA-based nanodevices.^{7,8} Others have been interested in studying the self-organization patterns of pH oscillators in unstirred reaction-diffusion systems. The FIS (ferrocyanide–iodate–sulfite) system is a typical pH oscillator that displays a variety of spatiotemporal behaviors such as self-replicating spots and stationary labyrinthine patterns.^{9,10} Recently, De Kepper and co-workers¹¹ have designed fronts, pulses, and Turing patterns in another pH-regulated system, the IO₃⁻–SO₃²⁻–thiourea reaction. Their design method should be applicable to other pH-oscillatory systems as well.

The reaction between hydrogen peroxide and thiosulfate has been found to display large amplitude ($\Delta T \sim 10$ – 20 °C) thermokinetic oscillations in the absence of a catalyst under quasiadiabatic conditions,¹² but no oscillations were found in homogeneous aqueous solution under isothermal conditions. The heat of reaction causes a change in the temperature, which generates the necessary feedbacks on the rates of key component reactions. Orbán and Epstein¹³ found that in the presence of trace amounts of Cu²⁺ (HPTCu system), the reaction exhibits

complex pH-regulated oscillations in a CSTR. Subsequently, Rábai and Epstein discovered that in alkaline medium the Cu(II)-catalyzed H₂O₂–S₂O₃²⁻ reaction shows oscillatory behavior under semibatch conditions, where a solution of S₂O₃²⁻ mixed with dilute NaOH is pumped at a constant rate into a mixture of H₂O₂ and Cu(II).¹⁴ Most recently, the HPTCu system has been reinvestigated with other experimental methods. One study¹⁵ found excitatory dynamics when the system was forced with base, acid, or other species. A second investigation¹⁶ revealed period-doubling and mixed mode oscillations as the flow rate was varied. The catalyst-free H₂O₂–S₂O₃²⁻–SO₃²⁻ reaction exhibits periodic and chaotic temporal pH-oscillations^{17,18} with temperature and flow rate as control parameters. Under special conditions, this system also shows temperature compensation.^{19,20}

In 1996, Kurin-Csörgei et al. proposed a mechanistic model²¹ for the HPTCu system based on a simple three-step model suggested by Schiller,²² which accounts for both the batch behavior and the oscillations and bistability observed in a CSTR. Subsequently, Rábai and Hanazaki¹⁷ made detailed numerical studies, which revealed some new features of the model. Their calculations showed that oscillatory behavior could also occur when the Cu²⁺-containing rate terms were omitted from the model. To date, however, this behavior has not been found experimentally. In both systems, the major overall processes are



The autocatalytic formation of H⁺ in reaction 2 provides the necessary positive feedback with reaction 3, which consumes H⁺, serving as the negative feedback for this pH-regulated oscillator. The further oxidation of tetrathionate by hydrogen peroxide in alkaline solution, which plays a key role in the

* To whom correspondence should be addressed. E-mail: gaoqy@cumt.edu.cn (Q.G.), epstein@brandeis.edu (I.R.E.).

[†] China University of Mining and Technology.

[‡] Brandeis University.

TABLE 1: Oscillatory Model for the HPTCu Reaction System

reactions	
M1	$\text{H}_2\text{O}_2 + \text{S}_2\text{O}_3^{2-} \rightarrow \text{HOS}_2\text{O}_3^- + \text{OH}^-$
M2	$\text{H}_2\text{O}_2 + \text{HOS}_2\text{O}_3^- \rightarrow 2\text{HSO}_3^- + \text{H}^+$
M3	$\text{S}_2\text{O}_3^{2-} + \text{HOS}_2\text{O}_3^- \rightarrow \text{S}_4\text{O}_6^{2-} + \text{OH}^-$
M4	$\text{S}_4\text{O}_6^{2-} + \text{H}_2\text{O}_2 \rightarrow 2\text{HOS}_2\text{O}_3^-$
M5	$\text{H}_2\text{O}_2 + \text{HSO}_3^- \rightarrow \text{SO}_4^{2-} + \text{H}_2\text{O} + \text{H}^+$
M6	$\text{H}_2\text{O}_2 + \text{SO}_3^{2-} \rightarrow \text{SO}_4^{2-} + \text{H}_2\text{O}$
M7	$\text{H}_2\text{O}_2 \leftrightarrow \text{HO}_2^- + \text{H}^+$
M8	$\text{H}_2\text{O} \leftrightarrow \text{OH}^- + \text{H}^+$
M9	$\text{HSO}_3^- \leftrightarrow \text{SO}_3^{2-} + \text{H}^+$
rate laws	rate constants
$\nu_1 = k_1[\text{H}_2\text{O}_2][\text{S}_2\text{O}_3^{2-}] + k_1'[\text{H}_2\text{O}_2][\text{S}_2\text{O}_3^{2-}][\text{Cu}^{2+}][\text{OH}^-]$	(k_i in $\text{M}^{-1} \text{s}^{-1}$ except k_7, k_8 , and k_9 in s^{-1} ; k_i' in $\text{M}^{-2} \text{s}^{-1}$, except k_1' in $\text{M}^{-3} \text{s}^{-1}$)
$\nu_2 = k_2[\text{H}_2\text{O}_2][\text{HOS}_2\text{O}_3^-]$	$k_1 = 0.019, k_1' = 3 \times 10^8$
$\nu_3 = k_3[\text{S}_2\text{O}_3^{2-}][\text{HOS}_2\text{O}_3^-] + k_3'[\text{S}_2\text{O}_3^{2-}][\text{HOS}_2\text{O}_3^-][\text{H}^+]$	$k_2 = 1$
$\nu_4 = k_4[\text{S}_4\text{O}_6^{2-}][\text{H}_2\text{O}_2] + k_4'[\text{S}_4\text{O}_6^{2-}][\text{H}_2\text{O}_2][\text{OH}^-]$	$k_3 = 50, k_3' = 10^5$
$\nu_5 = k_5[\text{HSO}_3^-][\text{H}_2\text{O}_2] + k_5'[\text{HSO}_3^-][\text{H}_2\text{O}_2][\text{H}^+]$	$k_4 = 0.0155, k_4' = 10^5$
$\nu_6 = k_6[\text{SO}_3^{2-}][\text{H}_2\text{O}_2]$	$k_5 = 7, k_5'$ variable; see text
$\nu_7 = k_7[\text{H}_2\text{O}_2]$	$k_6 = 0.2$
$\nu_{-7} = k_{-7}[\text{HO}_2^-][\text{H}^+]$	$k_7 = 0.003$
$\nu_8 = k_8[\text{H}_2\text{O}]$	$k_{-7} = 10^{10}$
$\nu_{-8} = k_{-8}[\text{OH}^-][\text{H}^+]$	$k_8[\text{H}_2\text{O}] = 0.001$
$\nu_9 = k_9[\text{HSO}_3^-]$	$k_{-8} = 10^{11}$
$\nu_{-9} = k_{-9}[\text{SO}_3^{2-}][\text{H}^+]$	$k_9 = 3000$
	$k_{-9} = 5 \times 10^{10}$

HPTCu system, has been studied by Voslar et al.²³ They propose a new kinetic model for the reaction and conclude that the real effect of copper(II) in the HPTCu system remains to be identified.

The above observations suggest two questions. (1) Can the periodic oscillations in the HPTCu system be driven into a chaotic state by using temperature as a bifurcation parameter? (2) Does the catalyst-free, isothermal H₂O₂–S₂O₃²⁻ reaction show the predicted oscillatory dynamics? To answer these questions, we have reinvestigated the HPTCu system in a CSTR.

II. Experimental Section

Materials. Reagent grade H₂O₂ (J&K, 30% solution), Na₂S₂O₃·5H₂O (Aldrich), CuSO₄ (Aldrich), and H₂SO₄ (Shanghai Suyi Chemical) were used without further purification. Doubly distilled water used in preparing solutions was first purged with N₂ to eliminate O₂ and CO₂. Hydrogen peroxide solution, standardized with permanganate solution, was prepared daily and kept in polyethylene bottles to retard decomposition.

Reactor. The CSTR (liquid volume 22.5 mL) was operated in isothermal mode and fed by a peristaltic pump (ISMATIC, Switzerland) through three inlet tubes (i.d. 1.3 mm). The reactor was equipped with a pH electrode and a thermistor to measure pH and temperature. pH-time data were collected with an ecorde201 (eDAQ, Australia) and recorded by a computer. A Teflon-covered magnetic stirrer (1 cm long) was used to ensure uniform mixing at about 700 rpm.

Computation. The simulations were carried out with a commercial software package (Berkeley Madonna,²⁴ error control parameter set at 10^{−10}) for stiff differential equations. The same results were obtained with the error control parameter set at 10^{−6} and 10^{−12} and with another stiff algorithm (Gear).

III. Simulation Results

The Model. Table 1 contains a version of the model developed by Kurin-Csörgei et al.²¹ for the copper-catalyzed isothermal reaction. The rate laws and the corresponding set of rate constants are also given in the table. In the simulations, the concentration of copper(II) ions is treated as a constant parameter, as in ref 21.

Calculated Results. For studying the effect of temperature on the dynamics, changing the temperature should influence the rates of all the component reactions, but we do not have data on their activation energies. Simulations show that the system is quite sensitive to the rate constant k_5' of composite reaction M5. We therefore choose to vary k_5' as a surrogate control parameter for temperature while keeping the other parameters constant. The values of k_2 and k_3 were selected to be 1 and 50 $\text{M}^{-2} \text{s}^{-1}$, respectively, both of which lie within the ranges previously used and are consistent with the ratio found to give oscillatory character ($k_3/k_2 = 40$ –100).²¹ The value of $k_7 = 0.003 \text{ s}^{-1}$ that we found to give the optimal range of complex oscillations is a bit lower than that employed in ref 21 ($k_7 = 0.022 \text{ s}^{-1}$), perhaps because our temperature range lies below 25 °C.

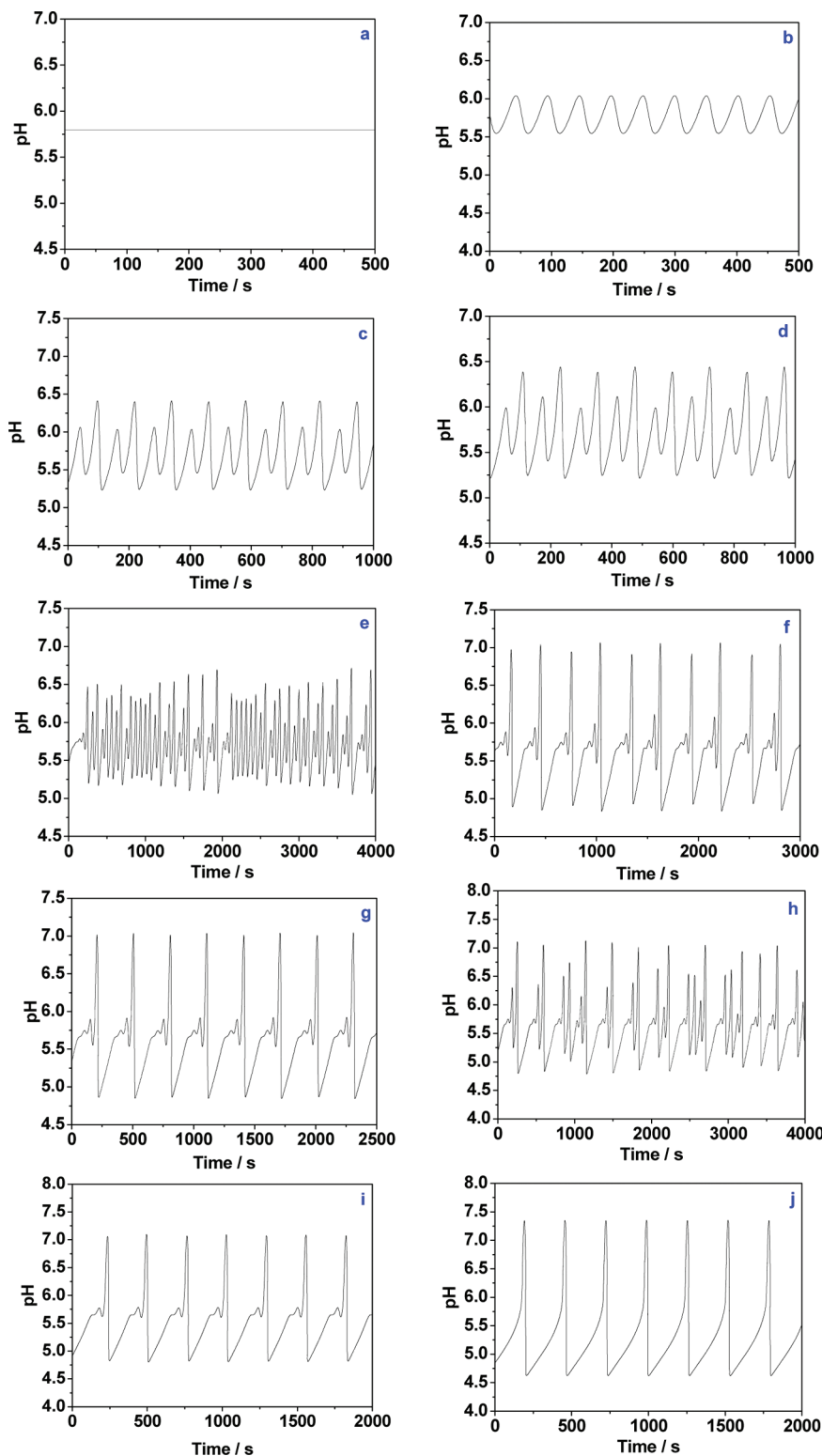


Figure 1. Calculated pH-time series based on the model in Table 1, with $k_5' =$ (a) $6.75 \times 10^5 \text{ M}^{-2} \text{ s}^{-1}$, steady state; (b) $7.25 \times 10^5 \text{ M}^{-2} \text{ s}^{-1}$, P1; (c) $8.53 \times 10^5 \text{ M}^{-2} \text{ s}^{-1}$, P2; (d) $8.61 \times 10^5 \text{ M}^{-2} \text{ s}^{-1}$, P4; (e) $8.79 \times 10^5 \text{ M}^{-2} \text{ s}^{-1}$, chaos; (f) $9.45 \times 10^5 \text{ M}^{-2} \text{ s}^{-1}$, $(1^3)^2$; (g) $9.52 \times 10^5 \text{ M}^{-2} \text{ s}^{-1}$, 1^2 ; (h) $1.01 \times 10^6 \text{ M}^{-2} \text{ s}^{-1}$, chaos; (i) $1.06 \times 10^6 \text{ M}^{-2} \text{ s}^{-1}$, 1^1 ; (j) $1.72 \times 10^6 \text{ M}^{-2} \text{ s}^{-1}$, P1. $[\text{H}_2\text{O}_2]_0 = 0.1 \text{ M}$, $[\text{Na}_2\text{S}_2\text{O}_3]_0 = 0.008 \text{ M}$, $[\text{H}^+]_0 = 10^{-3} \text{ M}$, $[\text{CuSO}_4]_0 = 5 \times 10^{-5} \text{ M}$, $k_0 = 3.6 \times 10^{-3} \text{ s}^{-1}$.

Simulated period-doubling, mixed-mode and aperiodic oscillations are shown in Figure 1. When we modulate the flow rate to about $3.6 \times 10^{-3} \text{ s}^{-1}$, we find the following sequence: steady state (a) \rightarrow P1 (high frequency) (b) \rightarrow P2 (c) \rightarrow P4 (d) \rightarrow chaos (e) \rightarrow mixed-mode oscillations (f, g) \rightarrow chaos (h) \rightarrow 1^1 (i) \rightarrow P1 (low frequency) (j). As we

increase k_5' at $k_0 = 3.6 \times 10^{-3} \text{ s}^{-1}$, we first observe simple small-amplitude oscillations, which then turn into small-amplitude period-doubling oscillations. P2 and P4 oscillations occur with $k_5' = 8.3 \times 10^5$ to $8.61 \times 10^5 \text{ M}^{-2} \text{ s}^{-1}$. The large-amplitude complex mixed-mode oscillations are found in a wide range, $k_5' = 9.4 \times 10^5$ to $1.7 \times 10^6 \text{ M}^{-2} \text{ s}^{-1}$, which

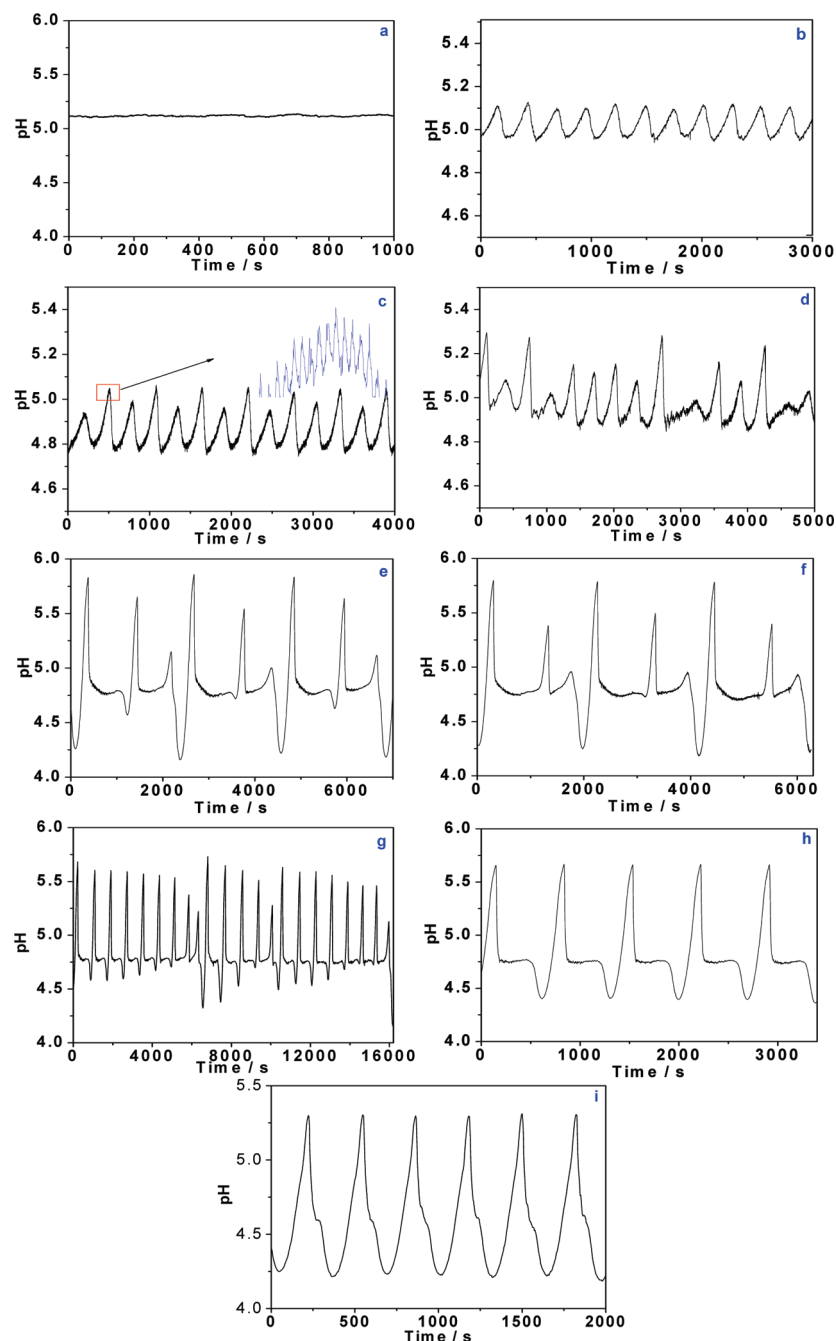


Figure 2. pH-time series measured in a CSTR at different temperatures. Experimental conditions are as in Figure 1, except $k_0 = 6.67 \times 10^{-4} \text{ s}^{-1}$, (a) 15.0, (b) 16.0, (c) 16.5, (d) 17.0, (e) 19.0, (f) 19.5, (g) 20.0, (h) 22.0, (i) 30.0.

contains many types of mixed-mode oscillations such as 1^3 , 1^2 , aperiodic oscillations, and 1^1 .

IV. Experimental Results

A. Bifurcation Dynamics in the Catalyst-Containing System. Enlightened by our simulations, we performed a series of systematic experiments, choosing the temperature as a control parameter and monitoring the pH of the system. The initial concentrations of the reactants were the same as those used in the simulations except for the flow rate ($k_0 = 6.67 \times 10^{-4} \text{ s}^{-1}$).

A similar bifurcation scenario is observed upon variation of the reaction temperature. As the temperature is increased, we observe the following regimes, which approximately accord with the simulations: At 15 °C, only a stable steady state is found (Figure 2a). A supercritical Hopf bifurcation occurs at 16 °C,

producing a small limit cycle. The simple small-amplitude oscillations shown in Figure 2b then undergo a bifurcation to complex oscillations (Figure 2c). Oddly, the P2 curves are not smooth, but are decorated with small-amplitude peaks. The inset in Figure 2c, which exhibits an enlarged peak, clearly shows these small high frequency oscillations. With a small further increase in temperature, the periodic oscillations give way to aperiodic oscillations. At still higher temperature, the small-amplitude peaks begin to vanish and persist only around pH 4.7 on the descending shoulder of large pH peaks. Next we observe the large-amplitude mixed-mode oscillation shown in Figure 2e, which has three sharp peaks and a small wide peak at the descending shoulder of the first large peak. We designate these as 1^3 (L^3)-type oscillations. One small peak disappears at 19.5 °C, resulting in 1^2 type oscillations. When the reaction

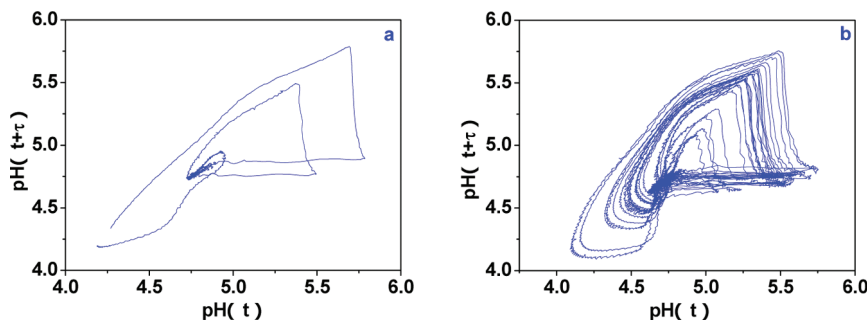


Figure 3. Attractors reconstructed ($\text{pH}(t)$ versus $\text{pH}(t + \tau)$) by the time-delay method from the data of (a) Figure 2f and (b) Figure 2g; optimal time delay $\tau = 30$ s.

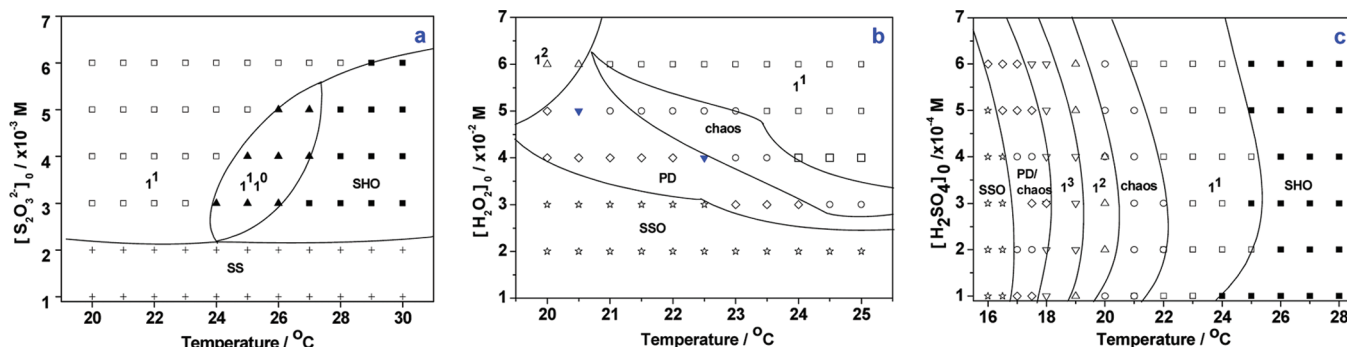


Figure 4. Phase diagrams of the HPTCu system in the temperature-[reactant]₀ plane. Fixed parameters: (a) $[\text{CuSO}_4]_0 = 5 \times 10^{-5}$ M, $[\text{H}_2\text{O}_2]_0 = 0.1$ M, $[\text{H}_2\text{SO}_4]_0 = 0.0005$ M, $k_0 = 6.67 \times 10^{-4}$ s⁻¹; (b) $[\text{CuSO}_4]_0 = 5 \times 10^{-5}$ M, $[\text{S}_2\text{O}_3^{2-}]_0 = 0.008$ M, $[\text{H}_2\text{O}_2]_0 = 0.0005$ M, $k_0 = 6.67 \times 10^{-4}$ s⁻¹; (c) $[\text{CuSO}_4]_0 = 5 \times 10^{-5}$ M, $[\text{S}_2\text{O}_3^{2-}]_0 = 0.008$ M, $[\text{H}_2\text{O}_2]_0 = 0.1$ M, $k_0 = 6.67 \times 10^{-4}$ s⁻¹. Symbols: ☆, SSO (simple small-amplitude oscillations); ◇, PD (period 2, small amplitude); ▼, period 4; ○, aperiodic oscillations; ▽, 1³; △, 1²; ▲, 1¹¹; □, 1¹; ■, SHO (simple high-amplitude oscillations); +, SS (steady state).

temperature reaches 20 °C, the mixed-mode oscillations again give way to aperiodic mixed-mode oscillations, as shown in Figure 2g. These turn into regular complex oscillations on further increasing the temperature, as seen in the 1¹ type oscillations of Figure 2h. These oscillations occur over a wide temperature range and evolve into simple large-amplitude oscillations [Figure 2i] at about 30.0 °C. The reverse route from simple high-amplitude periodic oscillations through mixed-mode oscillations and period-doubling oscillations to simple small-amplitude oscillations is also observed upon decreasing the temperature.

As the temperature is increased, the overall amplitude of oscillations first increases from 0.15 to 1.6 pH units. To examine the asymptotic dynamics, we use the time-delay method²⁵ to construct the attractor from the measured data. The attractor in Figure 3a exhibits three ribbonlike structures, which correspond to the three peaks seen in Figure 2f. Figure 2g represents an aperiodic mixed-mode regime of complex large-amplitude oscillations, and the attractor constructed from Figure 2g exhibits a corresponding chaotic structure.

B. Phase Diagram for the Catalyst-Containing System.

To investigate the combined effects of temperature and reactant concentrations, we carried out a series of experiments in which we also varied the concentrations of the reactants. The observed behavior is summarized in a set of temperature-[reactant]₀ phase diagrams. In each group of experiments, we fix the concentrations of the reactants and decrease the reaction temperature step by step. In the temperature- $[\text{Na}_2\text{S}_2\text{O}_3]_0$ phase diagram (Figure 4a), 1¹¹ type oscillations are found when the concentration of thiosulfate is between 0.003 and 0.005 M. When $[\text{H}_2\text{O}_2]_0 \leq 0.02$ M, the system shows only simple small-amplitude oscillations (Figure 4b). As the concentration of hydrogen peroxide is increased, the region of complex dynamics such as period-

doubling oscillations, aperiodic oscillations, and mixed-mode oscillations grows, and the period-doubling region shifts to lower temperature. When $[\text{H}_2\text{O}_2]_0 = 0.06$ mol·L⁻¹, only mixed-mode oscillations occur. We also fixed $[\text{H}_2\text{O}_2]_0$ and $[\text{S}_2\text{O}_3^{2-}]_0$ and determined the state of the system at various temperatures and $[\text{H}_2\text{SO}_4]_0$ (Figure 4c). We see that simple small-amplitude oscillations occur at low temperature. As the temperature is increased, the oscillatory amplitude becomes larger, and we see various phenomena such as simple, period-doubling and mixed-mode oscillations, which evolve to simple oscillations at still higher temperature.

C. Chemical Oscillations in the Catalyst-Free H_2O_2 - $\text{S}_2\text{O}_3^{2-}$ System. In their simulations, Rábai and Hanazaki¹⁷ found oscillations in the HPTCu model even when the Cu^{2+} -containing rate term was deleted from the mechanism. We studied the catalyst-free H_2O_2 - $\text{S}_2\text{O}_3^{2-}$ system with all experimental parameters the same as in Figure 2. At 28 °C, there are no oscillations (Figure 5a), though the catalyst-containing system gives simple oscillations under these conditions (Figure 5b). When $T < 25$ °C, small-amplitude high-frequency oscillations occur (Figure 5c). In the presence of copper, the system shows large amplitude oscillations modulated by smaller high frequency oscillations. By enlarging the small amplitude oscillations (Figure 5d), we see that these irregular oscillations are very similar to these found in the catalyst-free system.

When the Cu^{2+} -containing rate term in step M1 is omitted from the model shown in Table 1, small amplitude oscillations are obtained, as shown in Figure 5e with a low value of k_5' , which corresponds to the conditions in Figure 1. When k_5' is increased to 1.61×10^7 M⁻² s⁻¹, the system reaches the steady state shown in Figure 5f. These simulations thus give the same qualitative behavior as the experimental results. Thus Cu^{2+} is not essential for the oscillations. We further speculate that the

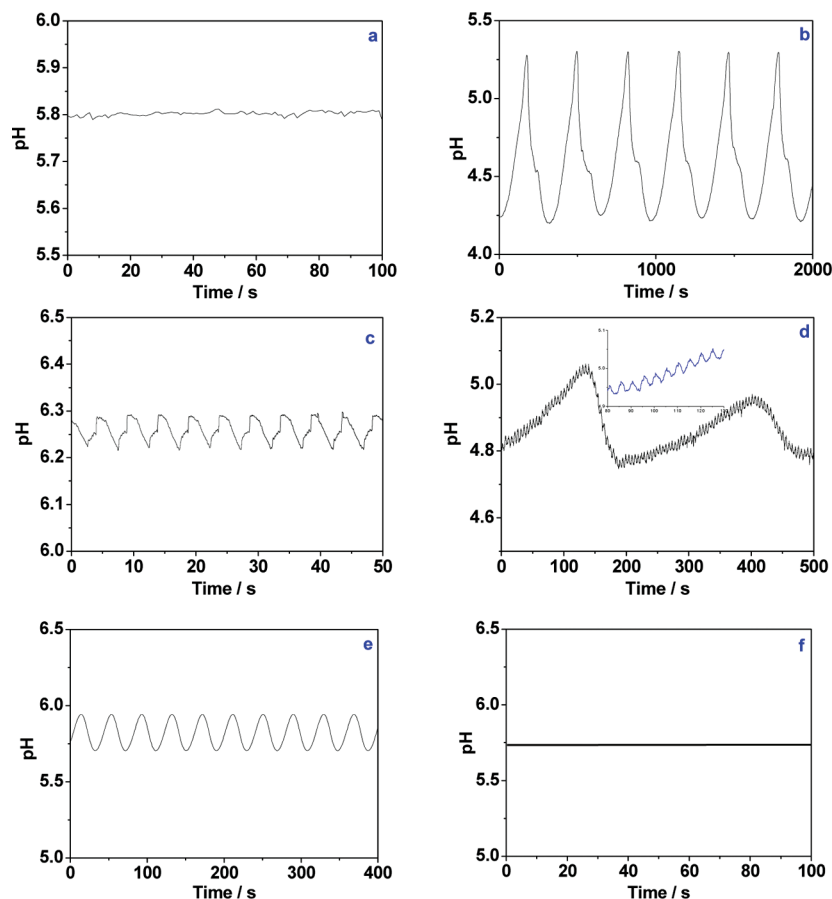


Figure 5. Oscillations in the Cu(II)-free and Cu(II)-catalyzed $\text{H}_2\text{O}_2\text{--S}_2\text{O}_3^{2-}\text{--H}_2\text{SO}_4$ systems. (a,c) pH-time series in the $\text{H}_2\text{O}_2\text{--S}_2\text{O}_3^{2-}\text{--H}_2\text{SO}_4$ system at 28.0 and 16.5 °C. (b,d) pH-time series in the $\text{H}_2\text{O}_2\text{--S}_2\text{O}_3^{2-}\text{--H}_2\text{SO}_4\text{--Cu}^{2+}$ system at 28.0 °C, 16.5 °C; (e,f) Calculated pH-time series in the catalyst-free system, $k_5' = 7.6 \times 10^5, 1.61 \times 10^7 \text{ M}^{-2} \text{ s}^{-1}$. Except for $[\text{CuSO}_4]_0$ in a and c, the reactant concentrations are the same as Figure 2.

high-frequency, small-amplitude irregular oscillations in the catalyst-containing reaction arise from the catalyst-free reaction between hydrogen peroxide and thiosulfate, while the high-amplitude, low-frequency oscillations are produced by the catalyst-mediated reaction.

V. Discussion and Conclusions

Clearly, our numerical exploration of temperature effects by varying a single rate constant, k_5' , is a crude approach. If we equate the lowest and highest k_5' values used in Figure 2 with temperatures of 15 and 22 °C, respectively, the upper and lower ends of the observed region of complex dynamics, the Arrhenius expression gives an activation energy of 90–100 kJ M^{-1} . This value may be a bit high, but it is not unreasonable so, especially since it serves as a proxy for increases in all the rate constants in the model. Of course, it would be preferable to incorporate realistic activation energies for most or all of the steps in the model, and we hope to be able to do so in the future as these quantities become available.

Rábai and Hanazaki's simulations¹⁷ suggest that, even in the absence of initial sulfite and catalyst (Cu^{2+}), the $\text{H}_2\text{O}_2\text{--S}_2\text{O}_3^{2-}$ reaction can display simple and complex oscillations. Here, we have obtained experimental oscillations in the catalyst-free $\text{H}_2\text{O}_2\text{--S}_2\text{O}_3^{2-}$ system. Under our experimental conditions, oscillations occur in a temperature range of 16–25 °C. We infer that the catalyst and sulfite modulate the feedback loop so as to enhance the oscillatory dynamics. The augmented production of HOS_2O_3^- from the Cu^{2+} catalyzed step M1 generates more

sulfite production in step M2 when the initial ratio of $[\text{H}_2\text{O}_2]_0$ to $[\text{S}_2\text{O}_3^{2-}]_0$ is high (>10), resulting in an acceleration of the proton-autocatalytic oxidation of sulfite (M5). The presence of initial sulfite directly forces the proton autocatalysis in step M5. Another question is whether there exists more than one feedback loop in the $\text{H}_2\text{O}_2\text{--S}_2\text{O}_3^{2-}$ system. Rábai and Hanazaki analyzed the model developed by Kurin-Csörgei et al.²¹ and proposed that the system has two paths for autocatalysis (M5 and M3 + M4), and two negative feedbacks (M1 and M2). One loop consists of M5 and M1, and the other of M3 + M4 and M2. A second model for the catalyst-free $\text{H}_2\text{O}_2\text{--S}_2\text{O}_3^{2-}\text{--SO}_3^{2-}$ reaction system proposed by Rábai and Hanazaki has two negative feedbacks (M1 and (4))



That work, however, did not yield oscillations in the absence of initial sulfite. The multiple feedbacks needed for complex oscillations and chaos appear to be inherent in the catalyst-free $\text{H}_2\text{O}_2\text{--S}_2\text{O}_3^{2-}$ system. Although the model proposed by Kurin-Csörgei et al.²¹ can predict the temperature-induced bifurcation dynamics, this behavior occurs at flow rates significantly different from those of our experiments. It will be necessary to study further the detailed mechanism of multiple feedbacks and Cu^{2+} effects in this system to obtain better agreement between simulation and experiment.

Our initial aim was to explore the effect of temperature on the $\text{H}_2\text{O}_2\text{--S}_2\text{O}_3^{2-}$ reaction catalyzed by cupric ions in a CSTR.

The use of temperature as a control parameter appears to be a powerful tool for obtaining mechanistic insights into this complex dynamical system. Period-doubling and mixed-mode oscillations were observed by increasing the reaction temperature. We found that, as suggested by earlier numerical work, the catalyst is not essential for oscillation. The catalyst-free system displays oscillations with small amplitude and high frequency. The $\text{H}_2\text{O}_2\text{--S}_2\text{O}_3^{2-}$ reaction system may be regarded as the core oscillator for both the HPTCu and $\text{H}_2\text{O}_2\text{--S}_2\text{O}_3^{2-}\text{--SO}_3^{2-}$ oscillators. The initial sulfite and Cu^{2+} -catalyst modulate the feedback loops to generate larger amplitude complex dynamics.

Acknowledgment. This work was supported in part by a Grant (CHE-0615507) from the U.S. National Science Foundation, Grants (20943005 and 50921002) from the National Science Foundation of China and a Grant (BK2007037) from the Research Foundation of Jiangsu Province. Q.G. is grateful for the financial support of the visiting program to Brandeis University from the Chinese Scholarship Council. We appreciate friendly discussions and help from Ms. Haimiao Liu.

References and Notes

- (1) Goldbeter, A. *Biochemical Oscillations and Cellular Rhythms: The Molecular Bases of Periodic and Chaotic Behaviour*; Cambridge University Press: Cambridge, U.K., 1996.
- (2) Glass, L.; Mackey, M. C. *From Clocks to Chaos: The Rhythms of Life*; Princeton University Press: Princeton, NJ, 1988.
- (3) Rábai, G.; Orbán, M.; Epstein, I. R. *Acc. Chem. Res.* **1990**, *23*, 258.
- (4) Yoshida, R.; Ichijo, H.; Hakuta, T.; Yamaguchi, T. *Macromol. Rapid Commun.* **1995**, *16*, 305.
- (5) Yoshida, R.; Tanaka, M.; Onodera, S.; Yamaguchi, T.; Kokufuta, E. *J. Phys. Chem. A* **2000**, *104*, 7549.
- (6) Misra, G. P.; Siegel, R. A. *J. Controlled Release* **2002**, *79*, 293.
- (7) Liedl, T.; Simmel, F. C. *Nano Lett.* **2005**, *5*, 1894.
- (8) Liedl, T.; Sobey, T. L.; Simmel, F. C. *Nano Today* **2007**, *2*, 36.
- (9) Lee, K. J.; McCormick, W. D.; Ouyang, Q.; Pearson, J. E.; Swinney, H. L. *Science* **1993**, *261*, 192.
- (10) Lee, K. J.; McCormick, W. D.; Pearson, J. E.; Swinney, H. L. *Nature* **1994**, *369*, 215.
- (11) Horváth, J.; Szalai, I.; De Kepper, P. *Science* **2009**, *324*, 772.
- (12) Chang, M.; Schmitz, R. A. *Chem. Eng. Sci.* **1975**, *30*, 21.
- (13) Orbán, M.; Epstein, I. R. *J. Am. Chem. Soc.* **1987**, *109*, 101.
- (14) Rábai, G.; Epstein, I. R. *J. Am. Chem. Soc.* **1992**, *114*, 1529.
- (15) Pesek, O.; Kofráňková, V.; Schreiberová, L.; Schreiber, I. *J. Phys. Chem. A* **2008**, *112*, 826.
- (16) Bakes, D.; Schreiberová, L.; Schreiber, I.; Hauser, M. J. B. *Chaos* **2008**, *18*, 015102.
- (17) Rábai, G.; Hanazaki, I. *J. Phys. Chem. A* **1999**, *103*, 7268.
- (18) Rábai, G.; Szanto, T. G.; Kovacs, K. *J. Phys. Chem. A* **2008**, *112*, 12007.
- (19) Rábai, G.; Hanazaki, I. *Chem. Commun.* **1999**, 1965.
- (20) Kovács, K. M.; Rábai, G. *Phys. Chem. Chem. Phys.* **2002**, *4*, 5265.
- (21) Kurin-Csörgei, K.; Orbán, M.; Rábai, G.; Epstein, I. R. *J. Chem. Soc., Faraday Trans.* **1996**, *92*, 2851.
- (22) Schiller, J. E. *Inorg. Chem.* **1987**, *26*, 948.
- (23) Voslar, M.; Matějka, P.; Schreiber, I. *Inorg. Chem.* **2006**, *45*, 2824.
- (24) Macey, R.; Oster, G. Differential equation solver: Berkeley Madonna, <http://www.berkeleymadonna.com/>, 1993–2001.
- (25) Takens, F. In *Dynamical Systems and Turbulence, Lecture Notes in Mathematics*; Rand, D. A., Young, L. S., Eds.; Springer-Verlag: Berlin, 1981; Vol. 898, pp 366–381.

JP102010K